Butenolide Inhibits Marine Fouling by Altering the Primary Metabolism of Three Target Organisms

Yi-Fan Zhang,[†] Huoming Zhang,[†,‡] Lisheng He,[†] Changdong Liu,[§] Ying Xu,[†] and Pei-Yuan Qian*,[†]

[†]KAUST Collaborative Research Program, Division of Life Science, Hong Kong University of Science and Technology, Hong Kong SAR, China

[‡]Department of Biology, Hong Kong Baptist University, Hong Kong SAR, China

[§]Division of Life Science, Hong Kong University of Science and Technology, Hong Kong SAR, China

Ⓢ *Supporting Information*

ABSTRACT: Butenolide is a very promising antifouling compound that inhibits ship hull fouling by a variety of marine organisms, but its antifouling mechanism was previously unknown. Here we report the first study of butenolide's molecular targets in three representative fouling organisms. In the barnacle *Balanus (=Amphibalanus) amphitrite*, butenolide bound to acetyl-CoA acetyltransferase 1 (ACAT1), which is involved in ketone body metabolism. Both the substrate and the product of ACAT1 increased larval settlement under butenolide treatment, suggesting its functional involvement. In the bryozoan *Bugula neritina*, butenolide bound to very long chain acyl-CoA dehydrogenase (ACADVL), actin, and glutathione *S*-transferases (GSTs). ACADVL is the first enzyme in the very long chain fatty acid β-oxidation pathway. The inhibition of this primary pathway for energy production in larvae by butenolide was supported by the finding that alternative energy sources (acetoacetate and pyruvate) increased larval attachment under butenolide treatment. In marine bacterium *Vibrio* sp. UST020129-010, butenolide bound to succinyl-CoA synthetase β subunit (SCSβ) and inhibited bacterial growth. ACAT1, ACADVL, and SCSβ are all involved in primary metabolism for energy production. These findings suggest that butenolide inhibits fouling by influencing the primary metabolism of target organisms.
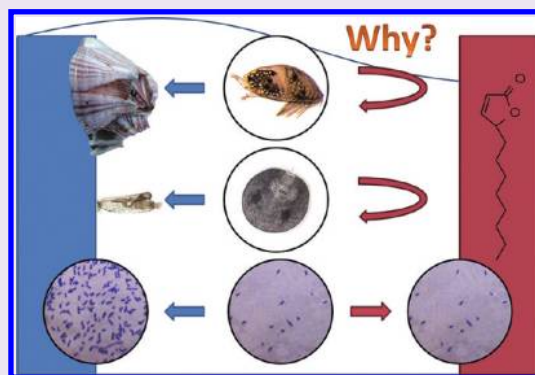
Biofouling is a serious problem in the marine industry and in aquaculture development. In the marine environment, submerged surfaces are colonized by biofoulers, that is, the marine organisms that attach to them. Biofoulers include such microfoulers as marine bacteria, algae, and protozoa and such macrofoulers as barnacles, bryozoans, and tubeworms.[1−3] They increase the weight, drag, and surface corrosion of ships, and lead to huge costs in maintaining mariculture systems.[4] Estimates suggest that fuel consumption would increase by as much as 40% if no antifouling measures were taken.[5] One of the most common antifouling methods is the coating of the ship hull with antifouling compounds. However, because biofoulers include distantly related organisms, finding a specific compound to target biofouling remains difficult. As a result, many widely used antifouling compounds are toxic.[6,7] The use of the toxic antifouling compound TBT, for example, caused significant ecological problems in the 1980s and 1990s,[8] suggesting the importance of learning more about the mechanism of these compounds before use.

The recently developed compound 5-octylfuran-2(5*H*)-one (referred to as butenolide **1**; Figure 1a) is a very promising antifouling agent that has great market potential because of its strong antifouling activity and simple structure.[9] In addition, it is derived from a natural product, and a recent comparison showed it to have the best species-selectivity ratio toward
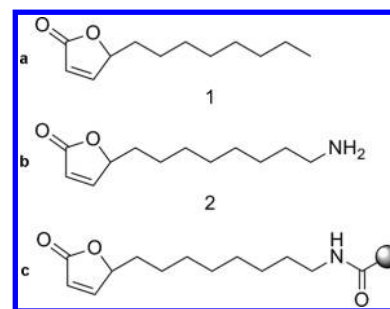

Figure 1. Chemical structures. (a) butenolide **1** [5-octylfuran-2(5*H*)-one], (b) butenolide **2** [5-(8-aminooctyl)furan-2(5*H*)-one], and (c) butenolide **2** conjugated to matrix (butenolide-matrix).

fouling organisms[10] and very high pharmaceutical ratios in target species,[9] thus suggesting a high degree of specificity. We believe environmental responsibility requires a better understanding of its pharmacology before its commercialization. Because butenolide **1** targets a broad spectrum of marine fouling species, its antifouling mechanism in multiple fouling

organisms requires investigation and comparison. We previously reported the proteomic, morphological, and behavioral changes induced by butenolide **1** in settlement-competent larvae of two fouling species,[11,12] which showed decreases in larval activities and regulations of energy- and stress-related proteins after butenolide **1** treatment. However, to date there have been no reports on the molecular target of butenolide **1**, which is crucial to understand its pharmacology. In the current study, its molecular targets were investigated in three representative fouling organisms: the barnacle *Balanus (=Amphibalanus) amphitrite*, the bryozoan *Bugula neritina* (bugula), and the marine bacterium *Vibrio* sp. UST020129-010. Barnacles and bryozoans of the genus *Bugula* are marine macrofouling invertebrates[3] and the major hard- and soft-fouling species, respectively. Their competent larvae, which are ready to settle, were used in this study. The marine biofilm-forming bacterium *Vibrio* sp. UST020129-010 represents the microfouling species.[3,13] These three organisms are distantly related in taxonomy, and each of them is representative. We identified the butenolide-binding proteins in these organisms, characterized two of them, and presented evidence to support their functional involvements in the antifouling effect of butenolide **1**. By comparing the mechanism in three organisms, this work suggests a possible general antifouling mechanism of butenolide **1**.

■ RESULTS AND DISCUSSION

Molecular Targets of Butenolide in *B. amphitrite*. In *B. amphitrite*, a protein with an apparent molecular mass of 40 kD specifically bound to the butenolide-matrix (Figures 1c and 2a). The protein was identified as acetyl-coenzyme A acetyltransferase (also referred to as thiolase) (Supplementary Table S1). The full-length cDNA of this protein was cloned (GenBank accession JN590268), and recombinant protein was expressed in *E. coli*. The recombinant protein could also be pulled down with the butenolide-matrix (Figure 2b), thus confirming the sequence of the butenolide-binding protein.

Eukaryotic thiolases are bidirectional enzymes that may be involved in different metabolic pathways (see Table 1 as an example).[14] Western blot showed that the butenolide-binding thiolase in *B. amphitrite* is located in the mitochondria/peroxisome fraction rather than in the cytosol (Figure 2f). MITOPROT prediction (http://ihg.gsf.de/ihg/mitoprot.html)[15] identified the cleavable amino-terminal mitochondrial targeting signal at its N-terminal (1-MAN-LLKNCRRMKPAARCLSTVTGLN-25). Its structure model and sequence analysis suggest that it can accommodate only four carbons (acetoacetyl coenzyme A) at most in its substrate binding pocket (Figure 3a−c). Together, these findings suggest that the butenolide-binding thiolase in *B. amphitrite* is acetyl-CoA acetyltransferase 1 (ACAT1 or T2 thiolase), an enzyme involved in ketone body synthesis and degradation (Table 1). Real-time polymerase chain reaction (PCR) analysis showed that its mRNA level was higher at the cyprid stage (ready to settle) than at the other developmental stage (nauplius II, nauplius VI, and juvenile stages) (Figure 2d), suggesting its importance to cyprids.

ACAT1 catalyzes the bidirectional reaction shown in Figure 2g. To confirm that ACAT1 is functionally involved in the antifouling activity of butenolide **1**, we tested the effect of several related metabolites on the cyprid larvae under butenolide **1** treatment by larval settlement assay (Figure 2h). Both the substrate and product of ACAT1 (acetyl-CoA and
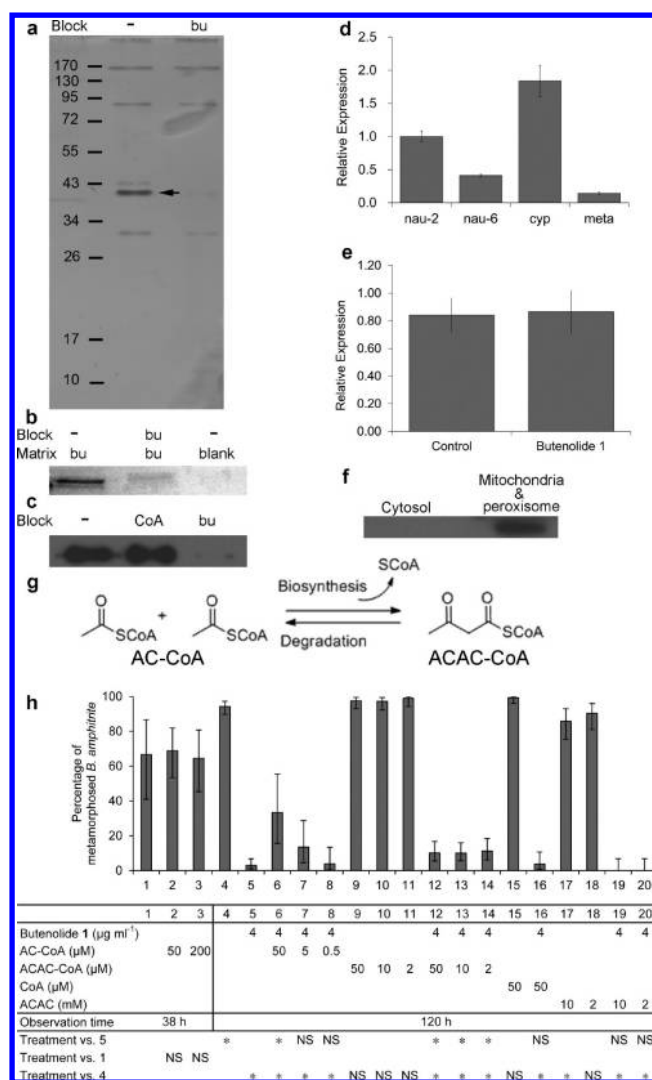

Figure 2. Butenolide's molecular target in *Balanus amphitrite*. (a) Silver stained SDS-PAGE gel of the proteins that were pulled down from the cell lysate with the butenolide-matrix. The lane (Block: bu) contains the proteins that bound to the butenolide-matrix in the presence of free butenolide **2** in the binding solution, thus serving as the competition controls for the lane with unblocked sample (Block: −). The 40 kD protein (arrow) was identified as thiolase by UPLC−MS/MS (see also Supplementary Table S1). (b) Coomassie blue stained SDS-PAGE gel of *B. amphitrite* thiolase recombinant protein, which was pulled down by the butenolide-matrix (Matrix: bu) or blank matrix (Matrix: blank, in which the matrix [Affi-Gel 10] was reacted with ethanolamine without butenolide **2** coating). The lane (Block: bu) is the competition control (explained in panel a). (c) Western blot analysis of *B. amphitrite* thiolase recombinant protein, which was pulled down by the butenolide-matrix. The sample with free coenzyme A in the solution (Block: CoA) had a thiolase amount similar to that of the sample without any blocking reagent (Block: −). (d,e) Real-time PCR analysis of the amount of thiolase mRNA, with 18S RNA as the control. The error bars represent standard errors. The vertical axis shows the relative amount of thiolase mRNA. (d) Relative amount of thiolase mRNA in several developmental stages of *B. amphitrite*. nau-2: nauplius II; nau-6: nauplius VI; cyp: cyprid; meta: metamorphosed juvenile. (e) Relative amount of thiolase mRNA in the cyprids after 9 h of butenolide **1** treatment compared with the 9 h control. (f) Subcellular localization of thiolase detected by Western blot. (g) The reaction catalyzed by thiolase with the C4 substrate/product. (h) The effect of several metabolites on the settlement of *B. amphitrite* with or without butenolide **1** treatment. The error bars represent the 95%

Figure 2. continued

confidence interval. *Significant difference at $p < 0.05$ in Fisher's exact test. NS: no significant difference. AC-CoA: acetyl-coenzyme A. ACAC-CoA: acetoacetyl-coenzyme A. CoA: coenzyme A. ACAC: acetoacetate.

acetoacetyl-CoA) significantly increased the percentage of successfully metamorphosed larvae under continuous butenolide **1** treatment. In contrast, without butenolide **1** treatment, neither acetyl-CoA nor acetoacetyl-CoA had a significant influence on the settlement rate of larvae. Other tested compounds such as coenzyme A and acetoacetate exhibited no significant rescue effects to larvae under butenolide **1** treatment. The antagonistic roles of ACAT1 substrate and product to the effect of butenolide **1** support that ACAT1 is the molecular target of butenolide **1** in *B. amphitrite*. Real-time PCR analysis showed that 9 h of butenolide **1** treatment had no significant impact on the amount of ACAT1 mRNA in cyprids compared to their control counterparts (Figure 2e), suggesting that the regulation of ACAT1 by butenolide **1** was at the functional level rather than at the expression level.

If the activity of ACAT1 was affected by butenolide **1**, then the ketone body metabolism would be altered in turn. As some densely compacted organs such as brains in higher organisms are unable to use the fatty acids generated from triglycerides,[16] the ketone bodies are transported into such tissues as alternative energy sources.[17] Triglycerides are the primary energy source for the nonfeeding *B. amphitrite* cyprid larvae,[18] and ketone bodies probably play similar roles in them as in higher organisms. An alteration in ketone body metabolism induced by butenolide **1** would probably affect the energy generation in densely compacted organs in *B. amphitrite*. This could be the reason why cyprids became less active and could not settle under butenolide **1** treatment.[12]

The predicted docking site of butenolide **1** on the structure model of *B. amphitrite* ACAT1 with the lowest free energy of binding is in the substrate binding pocket (Figure 3d). However, the binding between the butenolide-matrix and recombinant thiolase cannot be blocked by coenzyme A (Figure 2c). Further analysis is needed to identify the butenolide-ACAT1 interaction site.

Molecular Targets of Butenolide in *B. neritina*. Several proteins from the *B. neritina* cell lysate specifically bound to the butenolide-matrix (Figure 4a). They were identified with UPLC−MS/MS analysis (Supplementary Table S2): (1) the protein with an apparent molecular mass of 64 kD was similar to acyl-coenzyme A dehydrogenase (ACAD); (2) the protein

band with an apparent molecular mass of 40 kD contained a protein similar to actin; (3) the protein band with an apparent molecular mass of 24 kD contained two proteins similar to glutathione *S*-transferase (GST). The transcriptome database contains the full-length sequence of actin and the two GSTs. The 3′ terminal sequence of ACAD was cloned (GenBank accession JN602365).

ACAD family members have overlapping but distinct fatty acyl chain-length specificities and are located in either mitochondria or peroxisomes (see Table 2 as an example).[19−27]

The protein structure model and sequence analysis suggested that the butenolide-binding ACAD in *B. neritina* is mitochondrial very long chain acyl-coenzyme A dehydrogenase (ACADVL) (Figure 4b−d and Supporting Information), the enzyme that catalyzes the first step in very long chain fatty acid β-oxidation for energy generation.[19] The predicted docking site of butenolide **1** on its structure model with the lowest free energy of binding is in the substrate binding pocket (Figure 4e).

If the activity of an ACADVL was inhibited by butenolide **1**, then the lipid metabolism would be inhibited in turn, and the larvae would suffer from an energy shortage. Exogenous energy sources acetoacetate and pyruvate significantly increased the attachment rate of *B. neritina* under continuous butenolide **1** treatment. In contrast, without butenolide **1**, acetoacetate inhibited the settlement of *B. neritina* (Figure 4f). These results support the occurrence of energy shortage induced by butenolide **1**. The effects of acetyl-CoA and acetoacetyl-CoA were insignificant (Supplementary Figure S1), probably because the energy they provided were insufficient, as their concentrations were much lower than those of acetoacetate and pyruvate.

Surprisingly, Sudan Black B staining, which stains neutral fats, fatty acids, and phospholipids,[28] indicated that the butenolide **1**-treated bugula larvae were able to catalyze lipids at a rate similar to that of their control counterparts (Supplementary Figure S2), suggesting that there is another bugula ACAD(s) that catalyzes the dehydrogenation of very long chain fatty acyl-CoA in the presence of butenolide **1**. The only possible candidate that could be identified by blastp in the transcriptome database of *B. neritina* was the peroxisome enzyme acyl-coenzyme A oxidase (ACOX). Unlike ACADVL, ACOX does not pass the reducing power stored in fatty acids to the electron transport chain[27] for energy generation. It is likely to be the cause of the energy shortage in the butenolide **1**-treated larvae.

The attached *B. neritina* larvae under acetoacetate/butenolide **1** or pyruvate/butenolide **1** co-treatment died soon after the

Table 1. Summary of Thiolases in Human[14]

| thiolases in human	EC no.	location	MW[a] (kD)	function	mitochondria-targeting signal peptide
CT-thiolase (ACAT2, SOAT2)	EC 2.3.1.9	cytosol	41	steroid molecules synthesis	
A/B-thiolase (ACAA1)	EC 2.3.1.16	peroxisome	44 (α), 35 (β)	fatty acid degradation in peroxisome	signal peptide not for mitochondria
SCP2-thiolase	EC 2.3.1.176	peroxisome	59	oxidation of branched chain fatty acids, bile acid synthesis	
T1 thiolase (ACAA2)	EC 2.3.1.16	mitochondria	42	catalyzes the last step of the mitochondrial fatty acid β-oxidation spiral (C4-CoA specific)	no cleavable signal peptide
T2 thiolase (ACAT1)	EC 2.3.1.9	mitochondria	45	ketone body synthesis and degradation (C4-CoA specific)	cleavable signal peptide
$\alpha_4\beta_4$ thiolases	EC 2.3.1.16	mitochondria	45 (β)	fatty acid degradation (variable chain length)	

[a]Molecular weight.
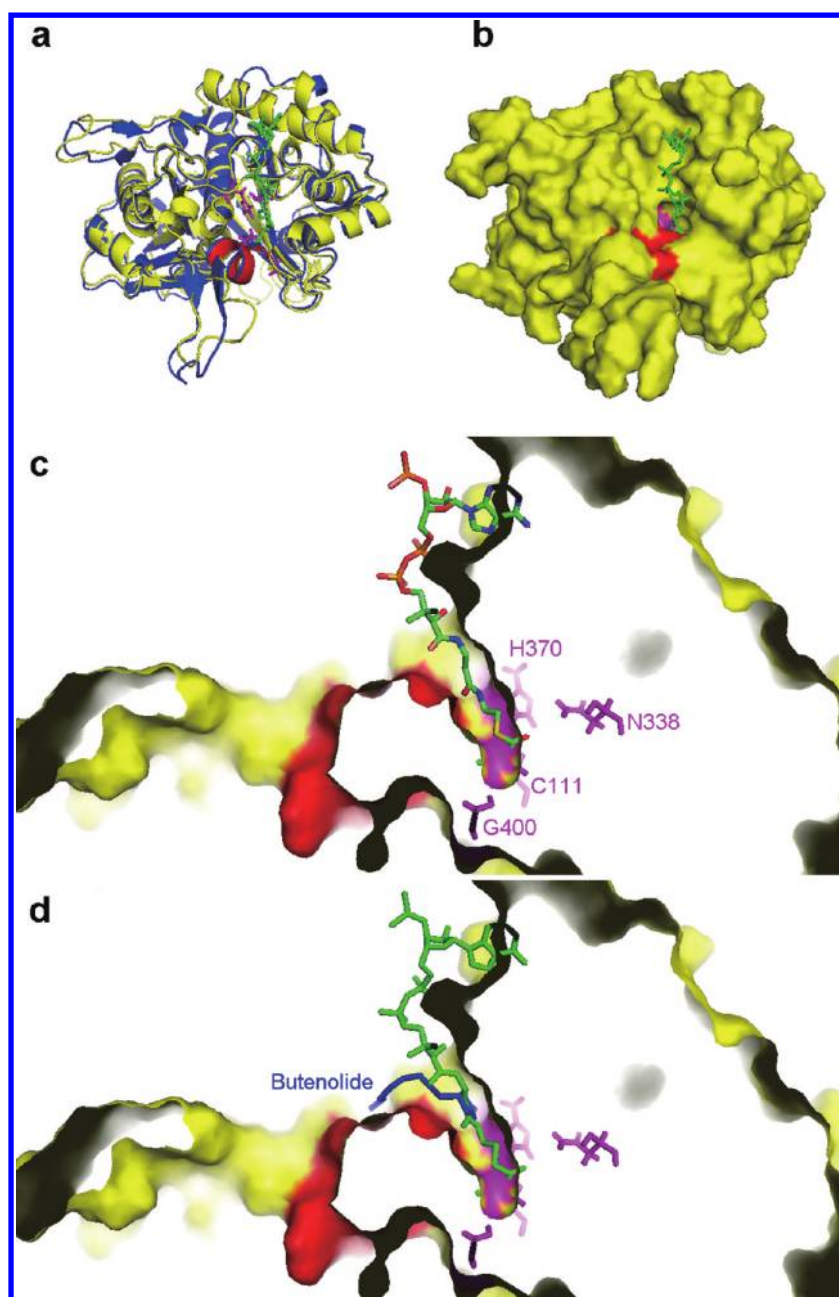
Figure 3. 3D structure model of butenolide-binding protein (ACAT1) in *B. amphitrite*. (a) Alignment of the model (yellow) with the *Zoogloea ramigera* biosynthetic thiolase structure (1M1T) (blue). The characteristic loop that restrains the substrate binding pocket is shown in red in the structure model of barnacle thiolase (residues 163-GIAYDGL-169, which is a superimposition of 142-TMIKDGL-148 in 1M1T). The residues in the putative active site of *B. amphitrite* thiolase (Cys-111, Asn-338, His-370, and Gly-400, which are superimpositions of residues Cys-89, Asn-316, His-348 and Gly-380 in 1M1T, respectively) are shown in magenta in the model. The substrate acetoacetyl-CoA is shown in green. (b) Surface view of the structure model of the *B. amphitrite* thiolase. The *Zoogloea ramigera* biosynthetic thiolase structure (1M1O) is not shown except for the substrate. The color schemes of the remainder are the same as those in panel a. (c) The shape of the substrate binding pocket near the active site. The color scheme for acetoacetyl-CoA is based on the elements: green (carbon), blue (nitrogen), red-purple (oxygen), yellow (sulfur), and orange (phosphorus). The hydrogen in the substrate is omitted. The color schemes for the others are the same as those in panel b. Note that the red loop on the protein model restrains the substrate binding pocket, such that the substrate with the longer carbon chain cannot be accommodated in the tight pocket. (d) Predicted docking site of butenolide **1** with the lowest free energy of binding. The butenolide **1** is shown in blue. The color schemes for the others are the same as those in panel b. Please refer to Supporting Information for further explanations.

attachment and never managed to start the metamorphosis successfully (Figure 4f). Their death occurred even sooner than that of the larvae treated with butenolide **1** alone. This was probably because of the functional change of another butenolide-binding protein − actin, although more direct evidence is needed to prove it. Actin was the strongest protein

band identified in the pull down assay with bugula. It is one of the major structural proteins of eukaryotic cells and plays a key role in muscle contraction and cell motility, as well as in many other cell processes and functions.[29] Actin exists as a variety of highly conserved isoforms that are functionally specialized and tissue-specific,[29] which may explain why these *B. neritina* larvae
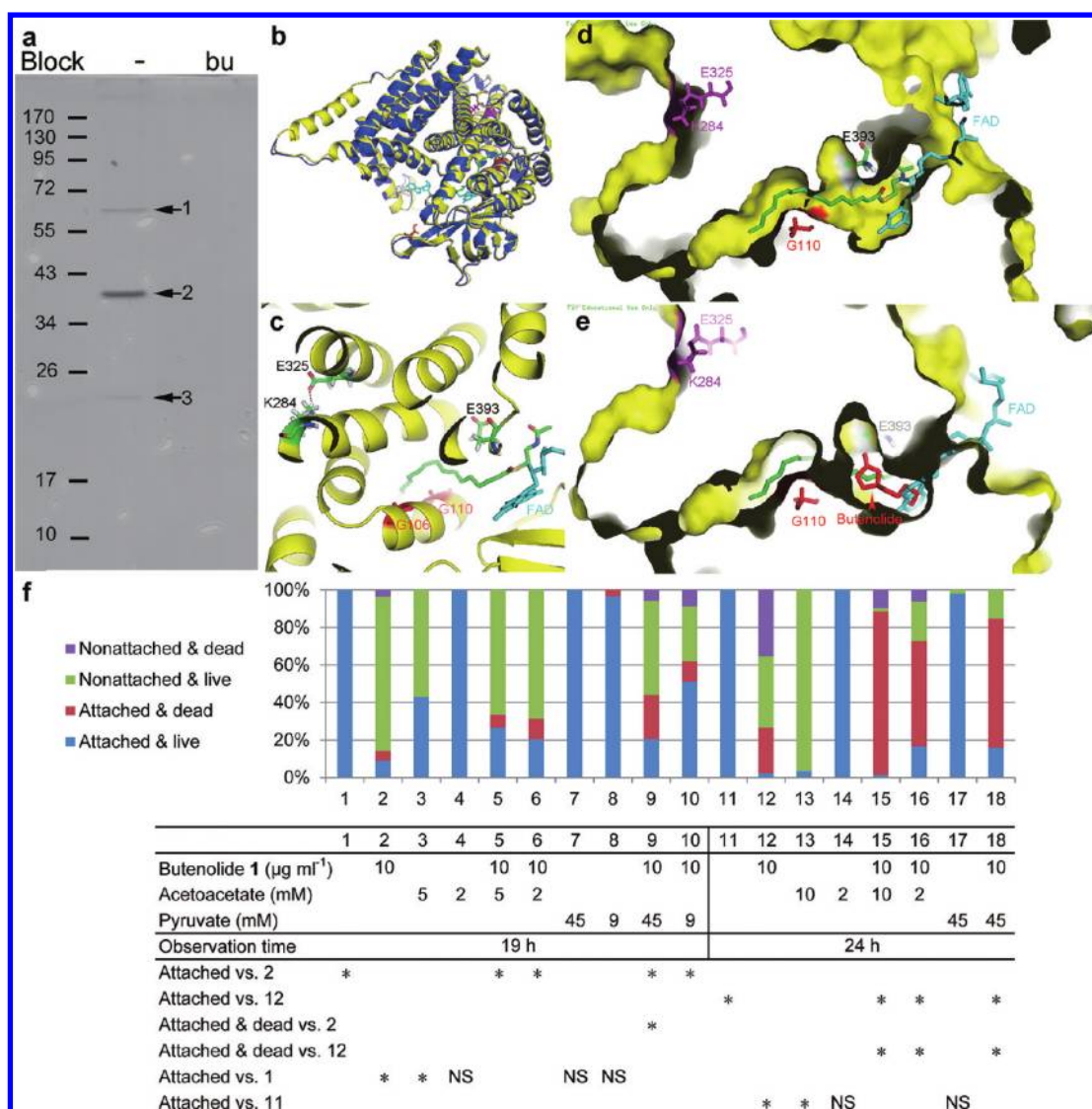
Figure 4. Butenolide's molecular target in *Bugula neritina*. (a) Silver stained SDS-PAGE gel of the proteins that were pulled down from the cell lysate with the butenolide-matrix. The lane (Block: bu) is the competition control (please refer to the legend of Figure 2a for explanations). UPLC−MS/ MS analysis (see also Supplementary Table S2) showed protein 1 to be very long chain-specific acyl-CoA dehydrogenase (mitochondrial), protein 2 to be actin, and protein band 3 to contain two glutathione S-transferases. (b−e) Structure model of protein 1 (ACADVL) in *B. neritina*. Please refer to Supporting Information for explanations. (b) Alignment of the model (yellow) with the human ACADVL (2UXW) (blue). The FAD (in cyan) and the truncated acyl-CoA substrate (trans-delta2-palmitenoyl-CoA) (green) are also shown. Note that Ser-201 (in orange) is far from the substrate, which is a characteristic of ACADVL (please refer to Supporting Information for explanations). (c) Cartoon view of the substrate binding site. Note that the putative salt bridge between Lys-284 and Glu-325 widens the substrate binding cavity, and Gly-106 and Gly-110 do not block the substrate binding pocket. Also note the presence of the putative catalytic base Glu-393 in the putative active site of *B. neritina* protein. The color schemes for the truncated C16-CoA, Lys-284, Glu-325, and Glu-393 are based on the elements: green (carbon), blue (nitrogen), red-purple (oxygen), yellow (sulfur), and gray (hydrogen, which is omitted in C16-CoA). Truncated FAD is depicted in cyan. (d) Shape of the substrate binding pocket. Note that the small side chain of Gly-110 does not block the substrate binding pocket. The color schemes for the Glu-393 and the C16-CoA substrate are based on the elements as in panel c. (e) Predicted docking site of butenolide with the lowest free energy of binding. The butenolide 1 is shown in red. The color schemes of the remainder are the same as those in panel d. (f) The effect of several metabolites on the settlement of *B. neritina* with or without butenolide 1 treatment. Please refer to Figure 2h for the labeling scheme and abbreviations.

had been swimming very well under butenolide 1 treatment and only died after attachment, as it is likely that butenolide 1 binds a specific actin isoform (or isoforms) that is involved in muscle contraction during metamorphosis but not in cilia movement during swimming. However, because of the high degree of sequence similarity between them, LC−MS/MS analysis was unable to identify the actin isoform.

Another butenolide-binding protein band in *B. neritina* contained two proteins similar to GST. The GST superfamily (EC 2.5.1.18) represents an integral part of the phase II

detoxification mechanism[30] and is likely to be involved in the butenolide 1 detoxification process. Some members of the GST superfamily play a prominent role in other physiological processes, such as the isolation and transportation of endogenous hydrophobic compounds in animal cells, including steroids, bilirubin, heme, and bile salts, and the synthesis of the localized hormones prostaglandins and leukotrienes (EC 5.3.99.2).[31] It is also possible that butenolide 1 interferes with these processes.

E

dx.doi.org/10.1021/cb200545s | *ACS Chem. Biol.* XXXX, XXX, XXX−XXX

Table 2. Summary of Acyl-CoA Dehydrogenases and Acyl-CoA Oxidases in Human[19−27]

	EC no.	location	form	optimal substrate	electron acceptor	MW[a] (kD)	function
ACADVL	EC 1.3.99.-	mitochondrial inner membrane	homodimer	16C straight chain acyl-CoA	ETF[b]	68	dehydrogenation of C14 to C18 acyl-CoA
ACAD9	EC 1.3.99.-	mitochondrial inner membrane	homodimer	unsaturated long chain acyl-CoA	ETF	69	dehydrogenation of unsaturated very long chain and saturated medium/very long chain acyl-CoA
ACADL	EC 1.3.99.13	mitochondrial matrix	homotetramer	14C straight chain acyl-CoA	ETF	48	dehydrogenation of C10 to C18 straight chain (saturated and some unsaturated) acyl-CoA
ACADM	EC 1.3.99.3	mitochondrial matrix	homotetramer	6C and 8C straight chain acyl-CoA	ETF	47	dehydrogenation of C6 to C12 straight chain acyl-CoA
ACADS	EC 1.3.99.2	mitochondrial matrix	homotetramer	4C straight chain acyl-CoA	ETF	44	dehydrogenation of C4 straight chain acyl-CoA
ACAD8	EC 1.3.99.-	mitochondrial matrix	homotetramer	isobutyryl-CoA	ETF	45	catabolism of the branched-chain amino acid valine
IVD	EC 1.3.99.10	mitochondrial matrix	homotetramer	3-methylbutanoyl-CoA	ETF	46	catalyzes the third step in leucine catabolism
GCDH	EC 1.3.99.7	mitochondrial matrix	homotetramer	glutaryl-CoA	ETF	48	oxidative decarboxylation of glutaryl-CoA to crotonyl-CoA and CO_2 in the degradative pathway of L-lysine, L-hydroxylysine, and L-tryptophan metabolism.
ACADSB	EC 1.3.99.-	mitochondrial matrix	homotetramer	the short branched chain acyl-CoA derivative, (S)-2-methylbutyryl-CoA	ETF	44	dehydrogenation of short branched chain acyl-CoA derivative, other 2-methyl branched chain substrates and short straight chain acyl-CoAs
ACOX1	EC 1.3.3.6	peroxisome matrix		very long chain acyl-CoA	O_2	74	first enzyme of the fatty acid β-oxidation pathway
ACOX2	EC 1.17.99.3	peroxisome matrix				77	oxidizes the CoA esters of the bile acid intermediates di- and trihydroxycholestanoic acids
ACOX3	EC 1.3.3.6	peroxisome				78	perhaps oxidizes the CoA esters of the bile acid intermediates dihydroxycholestanoic acids

[a]Molecular weight. [b]Electron transfer flavoprotein.

Butenolide-Binding Protein in Marine Bacteria *Vibrio* sp. UST020129-010. In antibacterial assay, butenolide **1** inhibited the growth of *Vibrio* sp. UST020129-010 (Figure 5b).
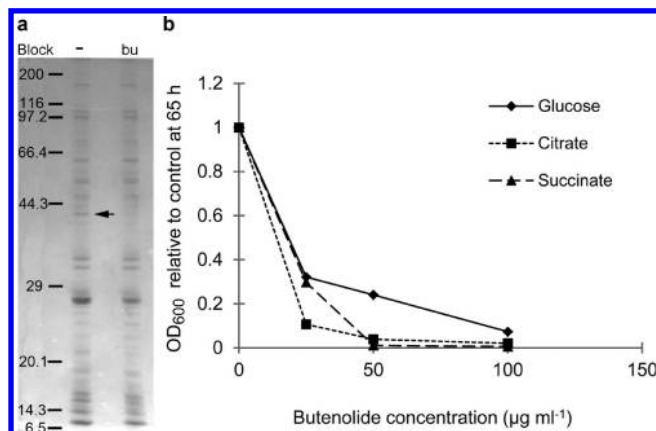

Figure 5. Butenolide's effect and binding target in *Vibrio* sp. UST020129-010. (a) Coomassie blue stained SDS-PAGE gel of the proteins that were pulled down from the cell lysate with the butenolide-matrix. The lane (Block: bu) is the competition controls (please refer to the legend of Figure 2a for explanations). The 42 kD protein (arrow) was identified as succinyl-CoA synthetase subunit beta (see also Supplementary Table S3). (b) Effect of butenolide **1** on the growth of marine bacteria *Vibrio* sp. UST020129-010 with different carbon sources.

The IC$_{50}$ was less than 25 μg mL^{-1} in the medium with either carbon source glucose (or citrate) or succinate. A 42 kD protein from its cell lysate specifically bound to the butenolide-matrix (Figure 5a). Mass spectrometric analysis identified two proteins in this band (Supplementary Table S3): succinyl-CoA synthetase (SCS) subunit beta (molecular weight 42 kD) and DNA-directed RNA polymerase subunit alpha (molecular weight 36 kD). Because the molecular weight of the latter differed from the apparent molecular weight of the band on the gel, we believe the former to be the butenolide-binding protein. SCS catalyzes the following reversible reaction: succinyl-CoA + Pi + NDP $\leftrightarrow$ succinate + CoA + NTP (where N denotes adenosine or guanosine). It is a step in the citric acid cycle and can also supply succinyl-CoA for heme synthesis and ketone body activation.[32] It is likely that butenolide **1** inhibits the function of SCS and, in turn, the energy production from the metabolism.

Among the six butenolide-binding proteins, two (ACAT1 and ACADVL) can bind acyl-CoA, two (actin and SCSβ[32]) can bind NTP, and two (GSTs) can bind glutathione. Although CoA did not block the interaction between ACAT1 and butenolide, the docking model with ACAT1 and ACADVL suggested that butenolide **1** may influence substrate (acyl-CoA) or coenzyme (FAD) binding (Figures 3d and 4e). Further analysis is needed to reveal butenolide's binding site on its targets. Three of these proteins (ACAT1, ACADVL, and SCSβ) are involved in the primary metabolism for energy production, and previous proteomic analysis of *B. amphitrite* and *B. neritina* has shown the regulation of energy metabolism-related proteins to be induced by butenolide **1** treatment.[11] In sum, these results suggest that butenolide **1**'s antifouling effect may stem largely from its influence on the primary metabolism.

As an antifouling compound, butenolide **1** was very effective in a 3-months antifouling test in the field and can be chemically

synthesized easily.[9] Its predicted no effect concentration (PNEC) is 0.168 μg L^{-1} according to OECD's guideline.[10] In a recent comparison with the most popular antifouling compounds, the comparably high species-selectivity ratio (0.635) of butenolide **1** suggested it to have good selectivity toward fouling organisms.[10] Toxicology studies in nontarget organisms zebrafish embryos and human cell lines suggested that the nonspecific effect of prolonged butenolide **1** treatment is through apoptosis.[10] The current pharmacology study is focused on the target organisms. No known proteins involved in cell cycle, cell proliferation, cell differentiation, cell death, or neuronal transmission were found to bind butenolide. It provides indirect but plausible explanations to previous findings: as butenolide **1** affected the primary metabolism of *B. amphitrite* and *B. neritina*, the expression/activities of energy-related proteins were regulated in response,[11,33] the treated animals became less active,[12] and a short exposure at antifouling concentrations would not kill them or greatly affect their competency to settle.[12] As a promising antifouling compound, the degradation and metabolism of butenolide **1** are yet to be characterized, and its compatibility with paint materials should also be well studied and optimized.

It is interesting to note that another group of antifouling furanones, which were halogenated and were first isolated as selective antifouling compounds from the red alga *Delisea pulchra*,[34] act by interfering with the interspecies communication of its target species *Serratia liquefaciens* MG1 and *Vibrio harveyi*.[35,36] Butenolide **1** has a side chain different from that of the halogenated furanones and has a different molecular mechanism. Another butenolide [2-(6-hydroxy-6-methyl-octyl)-2*H*-furan-5-one] has a chemical structure similar to that of butenolide **1** and exhibits novel antiparasitic activities specifically against *Trypanosoma brucei brucei*.[37] It is possible that the antiparasitic butenolide also acts by altering the primary metabolism of its target organism.

■ METHODS

Chemicals. Butenolide **1** [5-octylfuran-2(5*H*)-one] (Figure 1a) and its analogue butenolide **2** [5-(8-aminooctyl)furan-2(5*H*)-one] (Figure 1b) was synthesized by Shanghai Medicilon Inc.. Acetyl coenzyme A, acetoacetyl coenzyme A, coenzyme A, lithium acetoacetate, and pyruvate were obtained from Sigma-Aldrich.

Animals and Bacteria. The cyprid larvae of *Balanus amphitrite* and the swimming larvae of *Bugula neritina* were obtained as described in a previous report.[12] They were either used immediately in the experiments or stored in liquid nitrogen until usage. For the lipid staining of *B. neritina* (Supporting Information), the freshly released larvae and the larvae that had been prevented from settling by either continuous exposure to fluorescent light or the application of 10 μg mL^{-1} butenolide **1** were collected and processed.

The marine bacteria *Vibrio* sp. UST020129-010 were isolated from a 5-day-old natural biofilm developed in a polysterene Petri dish in subtidal seawater in Hong Kong (Fish Farm, Long Harbor, 22.45176780643477N, 114.34304237365723E) on January 29, 2002. They were amplified in a PY medium (0.5% peptone, 0.3% yeast extract in 0.22 μm filtered seawater) to the log phase before use.

Bioassays. Larval settlement assays were performed at RT in 24-well plates containing 1 mL of testing solution per well. The testing solutions were 0.22-μm-filtered seawater (FSW) containing compounds at indicated concentrations (Figures 2h, 4f and Supporting 1nformation). The tested concentrations of acetyl-CoA, acetoacetyl-CoA, CoA, and acetoacetate were close to their physiological concentrations in other organisms.[17,38−40] Fresh *B. amphitrite* cyprids (15−20 cyprids per well) or *B. neritina* swimming larvae (30−80 larvae per well) were incubated with the testing solutions and then observed under a dissecting microscope at indicated time (Figures 2h and 4f).

For *B. amphitrite*, the number of settled (attached and metamorphosed) larvae and swimming larvae were counted. For *B. neritina*, the larvae were categorized into four groups and counted: attached and live, attached and dead, nonattached and live, and nonattached and dead. The attached larvae were identified by shaking the plate and observed under the microscope. The living larvae were distinguished from the dead larvae by their dark color and intact body surface. More than 40 cyprids and more than 50 *B. neritina* swimming larvae were used in each test condition. The experiments were performed in triplicate.

In the antibacterial assay of *Vibrio* sp. UST020129-010, inoculums at the log phase were added into the 96-well plate with a dilution factor of 20. The assay medium was modified from Agata Czyż:[41] 6.05 g L^{-1} Tris, 3 g L^{-1} NaCl, 2 g L^{-1} KCl, 1 g L^{-1} NH_4Cl, 1.015 g L^{-1} $MgCl_2 \cdot 6H_2O$, 0.142 g L^{-1} Na_2SO_4, 0.128 g L^{-1} Na_2HPO_4, 10 g L^{-1} Casamino acids, 10 mg L^{-1} thiamine, and one of three carbon sources at 10 g L^{-1}, glucose, sodium succinate, or sodium citrate. Four butenolide **1** concentrations were tested: 0, 25, 50, and 100 μg mL^{-1}. The plate was incubated at 20 °C for 65 h before reading the absorbance at 600 nm. Each condition had six replicates.

Affinity Pull Down. A previous study showed that the functional group of the antifouling compound 5-octylfuran-2(5*H*)-one (butenolide **1**, Figure 1a) is located in the ring structure.[9] To identify the molecular target of butenolide **1**, its analogue butenolide **2** was synthesized for the affinity pull down because it contains a primary amine group that could be coupled to an Affi-Gel 10 matrix (Biorad) to afford the affinity matrix (Figure 1c), allowing the functional group to reach out to the proteins. Butenolide **2** also has much better water solubility than butenolide **1** and could be added into the protein lysate of the competition control. The butenolide-matrix coupling was performed according to Biorad's manual, and the reaction was stopped by incubation with ethanolamine. After washing, the affinity matrices were incubated with the protein sample, which was either a solubilized cell lysate or recombinant protein. In the competition control, competition with a soluble ligand was carried out by adding butenolide **2** (final concentration 0.4 mg mL^{-1}) or coenzyme A (final concentration 100 μM) to the protein sample before and during incubation with the affinity matrix to block the potential protein-affinity matrix interaction. After stringent washing in high ionic-strength solutions (500 mM NaCl in 1% Triton X100 in TBS), the proteins retained on the matrix were eluted by boiling in an SDS-sample buffer, separated by SDS-PAGE, visualized by silver stains or Coomassie stain, and analyzed by UPLC−MS/MS.

More specifically, to prepare the larval cell lysate, the larvae were homogenized in a homogenization buffer (320 mM sucrose, 10 mM Tris·Cl [pH 7.4], Roche's Complete Protease Inhibitor Cocktail) with a Dounce homogenizer on ice. To prepare the cell lysate of *Vibrio* sp. UST020129-010, the bacteria were amplified in a PY medium to the log phase and lysed by incubating with lysozyme (1 mg mL^{-1}) in PBS (pH 6.0) at 37 °C for 30 min. The cell lysates were centrifuged at 600 × g for 5 min at 4 °C, and the supernatant was collected. The total protein concentration in the supernatant was determined with a Bradford protein assay kit (Biorad). The lysate (10 mg of protein from the target organism) or recombinant protein (0.01 mg) was then solubilized in the binding buffer (TBS [pH 7.4], 1% Triton X100, complete protease inhibitor cocktail [Roche]) for 2 h at 4 °C. The solubilized protein samples were centrifuged at 13,000 × g for 20 min at 4 °C, and then the supernatant with/without blocking was incubated with the butenolide-matrix on a rotator mixer at 4 °C for 4 h at 30 μL butenolide-matrix per 4 mg protein in the cell lysate or per 10 μg recombinant protein. The butenolide-matrix was precipitated by centrifugation at 1,000 × g for 1 min at 4 °C, washed with 500 mM NaCl-supplemented binding buffer, and incubated with Laemmli sample buffer at 95 °C for 10 min to elute the retained proteins. The eluted protein samples were analyzed with 12% Tris-glycine gel electrophoresis and then processed to Western blot with our purified rabbit antithiolase polyclonal antibody or stained by silver reagents for imaging or with G-250 Colloidal Coomassie for both imaging and MS analysis. The proteins that specifically bind butenolide were detected and cut from the gel, processed, and analyzed by UPLC−MS/MS, as

previously described.[42] Our customized *B. amphitrite* database[43] and *B. neritina* database (submitted to NCBI, accession number SRA010777.2)[44] were used in the Mascot search for the pull down assay in *B. amphitrite* and *B. neritina*, respectively. Because there is a lack of *Vibrio* sp. UST020129-010 specific proteins database, the protein database of *Vibrio harveyi* ATCC BAA-1116 was used to analyze the MS/MS data of the *Vibrio* sp. UST020129-010 proteins as their 16S rRNA partial sequence and polymerase beta subunit (rpoB) gene partial sequence were very similar.

RNA Extraction, cDNA Synthesis, Real-Time PCR, and Gene Cloning. Total RNA extraction, cDNA synthesis with the Oligo-dT(18) primer, real-time PCR analysis with the *B. amphitrite* 18S RNA gene as the reference gene, and gene cloning with specific primers (Supplementary Table S4) were performed using the same technique as that described in a previous study.[45] For the real-time PCR, RNA was extracted from cyprids that had been treated for 9 h with butenolide **1** at 4 μg mL^{-1}, from cyprids in the 9 h control (DMSO as the solvent control), and from nauplii II, nauplii VI, fresh cyprids, and the juvenile (metamorphosed) stage of barnacles, respectively.

■ ASSOCIATED CONTENT

Ⓢ Supporting Information

This material is available free of charge *via* the Internet at http://pubs.acs.org.

■ AUTHOR INFORMATION

Corresponding Author

*E-mail: boqianpy@ust.hk.

Notes

The authors declare no competing financial interest.

■ ACKNOWLEDGMENTS

■ REFERENCES

(1) Dobretsov, S., Dahms, H.-U., and Qian, P.-Y. (2006) Inhibition of biofouling by marine microorganisms and their metabolites. *Biofouling* 22, 43−54.

(2) Wahl, M. (1989) Marine epibiosis. 1. Fouling and antifouling: some basic aspects. *Mar. Ecol.: Prog. Ser. 58*, 175−189.

(3) Callow, M. E., and Callow, J. A. (2002) Marine biofouling: a sticky problem. *Biologist 49*, 10−14.

(4) Chambers, L. D., Stokes, K. R., Walsh, F. C., and Wood, R. J. K. (2006) Modern approaches to marine antifouling coatings. *Surf. Coat. Technol. 201*, 3642−3652.

(5) Yebra, D. M., Kiil, S., and Dam-Johansen, K. (2004) Antifouling technology—past, present and future steps towards efficient and environmentally friendly antifouling coatings. *Prog. Org. Coat. 50*, 75−104.

(6) Flemming, C. A., and Trevors, J. T. (1989) Copper toxicity and chemistry in the environment: a review. *Water, Air, Soil Poll. 44*, 143−158.

(7) Iwao, O. (2003) Organotin antifouling paints and their alternatives. *Appl. Organomet. Chem. 17*, 81−105.

(8) Svavarsson, J. (2000) Imposex in the Dogwhelk (Nucella lapillus) due to TBT contamination: improvement at high latitudes. *Mar. Pollut. Bull. 40*, 893−897.

(9) Xu, Y., He, H., Schulz, S., Liu, X., Fusetani, N., Xiong, H., Xiao, X., and Qian, P.-Y. (2010) Potent antifouling compounds produced by marine Streptomyces. *Bioresour. Technol. 101*, 1331−1336.

(10) Zhang, Y.-F., Xiao, K., Chandramouli, K. H., Xu, Y., Pan, K., Wang, W.-X., and Qian, P.-Y. (2011) Acute toxicity of the antifouling compound butenolide in non-target organisms. *PLoS ONE 6*, e23803.

(11) Zhang, Y., Xu, Y., Arellano, S. M., Xiao, K., and Qian, P.-Y. (2010) Comparative proteome and phosphoproteome analyses during cyprid development of the barnacle Balanus (=Amphibalanus) amphitrite. *J. Proteome Res. 9*, 3146−3157.

(12) Zhang, Y.-F., Wang, G.-C., Ying, X., Sougrat, R., and Qian, P.-Y. (2011) The effect of butenolide on behavioral and morphological changes in two marine fouling species, the barnacle Balanus amphitrite and the bryozoan Bugula neritina. *Biofouling 27*, 467−475.

(13) Qian, P.-Y., Rittschof, D., Sreedhar, B., and Chia, F. S. (1999) Macrofouling in unidirectional flow: miniature pipes as experimental models for studying the effects of hydrodynamics on invertebrate larval settlement. *Mar. Ecol.: Prog. Ser. 191*, 141−151.

(14) Merilainen, G., Poikela, V., Kursula, P., and Wierenga, R. K. (2009) The thiolase reaction mechanism: the importance of Asn316 and His348 for stabilizing the enolate intermediate of the Claisen condensation. *Biochemistry 48*, 11011−11025.

(15) Claros, M. G., and Vincens, P. (1996) Computational method to predict mitochondrially imported proteins and their targeting Sequences. *Eur. J. Biochem. 241*, 779−786.

(16) Berg, J. M., Tymoczko, J. L., Stryer, L. (2002) *Biochemistry*, 5th ed., pp 851, W. H. Freeman and Company, New York.

(17) Laffel, L. (1999) Ketone bodies: a review of physiology, pathophysiology and application of monitoring to diabetes. *Diabetes Metab. Res. 15*, 412−426.

(18) Thiyagarajan, V., Harder, T., and Qian, P.-Y. (2002) Relationship between cyprid energy reserves and metamorphosis in the barnacle Balanus amphitrite Darwin (Cirripedia; Thoracica). *J. Exp. Mar. Biol. Ecol. 280*, 79−93.

(19) McAndrew, R. P., Wang, Y., Mohsen, A.-W., He, M., Vockley, J., and Kim, J.-J. P. (2008) Structural basis for substrate fatty acyl chain specificity. *J. Biol. Chem. 283*, 9435−9443.

(20) Ensenauer, R., He, M., Willard, J.-M., Goetzman, E. S., Corydon, T. J., Vandahl, B. B., Mohsen, A.-W., Isaya, G., and Vockley, J. (2005) Human acyl-CoA dehydrogenase-9 plays a novel role in the mitochondrial beta-oxidation of unsaturated fatty acids. *J. Biol. Chem. 280*, 32309−32316.

(21) Ikeda, Y., Okamura-Ikeda, K., and Tanaka, K. (1985) Purification and characterization of short-chain, medium-chain, and long-chain acyl-CoA dehydrogenases from rat liver mitochondria. Isolation of the holo- and apoenzymes and conversion of the apoenzyme to the holoenzyme. *J. Biol. Chem. 260*, 1311−1325.

(22) Izai, K., Uchida, Y., Orii, T., Yamamoto, S., and Hashimoto, T. (1992) Novel fatty acid beta-oxidation enzymes in rat liver mitochondria. I. Purification and properties of very-long-chain acyl-coenzyme A dehydrogenase. *J. Biol. Chem. 267*, 1027−1033.

(23) Oey, N. A., Ruiter, J. P. N, Ijlst, L., Attie-Bitach, T., Vekemans, M., Wanders, R. J. A., and Wijburg, F. A. (2006) Acyl-CoA dehydrogenase 9 (ACAD 9) is the long-chain acyl-CoA dehydrogenase in human embryonic and fetal brain. *Biochem. Biophys. Res. Commun. 346*, 33−37.

(24) Aoyama, T., Tsushima, K., Souri, M., Kamijo, T., Suzuki, Y., Shimozawa, N., Orii, T., and Hashimoto, T. (1994) Molecular cloning and functional expression of a human peroxisomal acyl-coenzyme A oxidase. *Biochem. Biophys. Res. Commun. 198*, 1113−1118.

(25) Baumgart, E., Vanhooren, J., Fransen, M., Marynen, P., Puype, M., Vandekerckhove, J., Leunissen, J. A. M., Fahimi, H. D., Mannaerts, G. P., and Van Veldhoven, P. P. (1996) Molecular characterization of the human peroxisomal branchedchain acyl-CoA oxidase: cDNA cloning, chromosomal assignment, tissue distribution, and evidence for the absence of the protein in Zellweger syndrome. *Proc. Nat. Acad. Sci. U.S.A. 93*, 13748−13753.

(26) Vanhooren, J. C., Marynen, P., Mannaerts, G. P., and Van Veldhoven, P. P. (1997) Evidence for the existence of a pristanoyl-CoA oxidase gene in man. *Biochem. J. 325*, 593−599.

(27) Tokuoka, K., Nakajima, Y., Hirotsu, K., Miyahara, I., Nishina, Y., Shiga, K., Tamaoki, H., Setoyama, C., Tojo, H., and Miura, R. (2006) Three-dimensional structure of rat-liver acyl-CoA oxidase in complex with a fatty acid: insights into substrate-recognition and reactivity toward molecular oxygen. *J. Biochem. 139*, 789−795.

(28) Bancroft, J. D., Stevens, A. (1990) *Theory and Practice of Histological Techniques*, 3rd ed., pp 221, Churchill Livingstone Elsevier Limited. Edinburgh, New York.

(29) Khaitlina, S. Y. (2001) Functional specificity of actin isoforms, in *International Review of Cytology* (Jeon, K. W., Ed.) pp 35−98, Academic Press, San Diego.

(30) Dirr, H., Reinemer, P., and Huber, R. (1994) X-ray crystal structures of cytosolic glutathione S-transferases. *Eur. J. Biochem. 220*, 645−661.

(31) Blanchette, B., Feng, X., and Singh, B. (2007) Marine glutathione S-transferases. *Mar. Biotechnol. 9*, 513−542.

(32) Fraser, M. E., James, M. N. G., Bridger, W. A., and Wolodko, W. T. (1999) A detailed structural description of Escherichia coli succinyl-CoA synthetase. *J. Mol. Biol. 285*, 1633−1653.

(33) Qian, P.-Y., Wong, Y. H., and Zhang, Y. (2010) Changes in the proteome and phosphoproteome expression in the bryozoan Bugula neritina larvae in response to the antifouling agent butenolide. *Proteomics 10*, 3435−3446.

(34) De Nys, R., Steinberg, P. D., Willemsen, P., Dworjanyn, S. A., Gabelish, C. L., and King, R. J. (1995) Broad spectrum effects of secondary metabolites from the red alga delisea pulchra in antifouling assays. *Biofouling 8*, 259−271.

(35) Rasmussen, T. B., Manefield, M., Andersen, J. B., Eberl, L., Anthoni, U., Christophersen, C., Steinberg, P., Kjelleberg, S., and Givskov, M. (2000) How Delisea pulchra furanones affect quorum sensing and swarming motility in Serratia liquefaciens MG1. *Microbiology 146*, 3237−3244.

(36) Ren, D., Sims, J. J., and Wood, T. K. (2001) Inhibition of biofilm formation and swarming of Escherichia coli by (5Z)-4-bromo-5-(bromomethylene)-3-butyl-2(5H)-furanone. *Environ. Microbiol. 3*, 731−736.

(37) Pimentel-Elardo, S. M., Kozytska, S., Bugni, T. S., Ireland, C. M., Moll, H., and Hentschel, U. (2010) Anti-parasitic compounds from Streptomyces sp. strains isolated from mediterranean sponges. *Mar. Drugs 8*, 373−380.

(38) Takamura, Y., and Nomura, G. (1988) Changes in the intracellular concentration of acetyl-CoA and malonyl-CoA in relation to the carbon and energy metabolism of Escherichia coli K12. *J. Gen. Microbiol. 134*, 2249−2253.

(39) Menahan, L. A., Hron, W. T., Hinkelman, D. G., and Miziorko, H. M. (1981) Interrelationships between 3-hydroxy-3-methylglutaryl-CoA synthase, acetoacetyl-CoA and ketogenesis. *Eur. J. Biochem. 119*, 287−294.

(40) Voltti, H., Savolainen, M. J., Jauhonen, V. P., and Hassinen, I. E. (1979) Clofibrate-induced increase in coenzyme A concentration in rat tissues. *Biochem. J. 182*, 95−102.

(41) Czyz, A., Zielke, R., Konopa, G., and Wegrzyn, G. (2001) A Vibrio harveyi insertional mutant in the cgtA (obg, yhbZ) gene, whose homologues are present in diverse organisms ranging from bacteria to humans and are essential genes in many bacterial species. *Microbiology 147*, 183−191.

(42) Wong, Y. H., Arellano, S. M., Zhang, H., Ravasi, T., and Qian, P.-Y. (2010) Dependency on de novo protein synthesis and proteomic changes during metamorphosis of the marine bryozoan Bugula neritina. *Proteome. Sci. 8*, 25.

(43) Chen, Z.-F., Matsumura, K., Wang, H., Arellano, S. M., Yan, X., Alam, I., Archer, J. A. C., Bajic, V. B., and Qian, P.-Y. (2011) Toward an Understanding of the molecular mechanisms of barnacle larval

settlement: a comparative transcriptomic approach. *PLoS ONE 6*, e22913.

(44) Wang, H., Zhang, H., Wong, Y. H., Voolstra, C., Ravasi, T., B. Bajic, V., and Qian, P.-Y. (2010) Rapid transcriptome and proteome profiling of a non-model marine invertebrate, Bugula neritina. *Proteomics 10*, 2972−2981.

(45) Wang, H., and Qian, P.-Y. (2010) Involvement of a novel p38 mitogen-activated protein kinase in larval metamorphosis of the polychaete Hydroides elegans (Haswell). *J. Exp. Zool., Part B 314B*, 390−402.

J

dx.doi.org/10.1021/cb200545s | *ACS Chem. Biol.* XXXX, XXX, XXX−XXX